

# Combining absorbing and nonreflecting boundary conditions for elastic wave simulation

Zaiming Jiang, John C. Bancroft, and Laurence R. Lines

## ABSTRACT

The absorbing boundary conditions and the nonreflecting boundary condition are two of the most popular solutions to the computational boundary condition problem. We report our implementations of these boundary conditions within our staggered-grid finite-difference applications and describe their features. Then we present a method combining the absorbing boundary conditions and the nonreflecting boundary condition.

## INTRODUCTION

Computational boundary condition problems have been a persistent topic in the field of wave phenomena modelling. Migration algorithms also have to deal with boundaries.

There are a lot of solutions to the boundary condition problems. The most cited method about boundary conditions is the “absorbing boundary conditions” proposed by Engquist and Majda (1977), and Clayton and Engquist (1977). Another popular method called “nonreflecting boundary condition” was presented by Cerjan, Kosloff, Kosloff, and Reshef in 1985. There are some other solutions as well, such as “transparent boundary” by Long and Liow (1990) and “perfectly matched layer” method by Collino and Tsogka (2001).

This report reviews the absorbing and nonreflecting boundary conditions first, and then presents our combined boundary conditions.

## RIGID BOUNDARY CONDITIONS

Elastic modelling method we are using is base on the Madariaga-Virieux staggered-grid scheme (Virieux, 1986).

To illustrate the boundary conditions, a subsurface model, which contains a point diffractor in a homogenous medium in  $x-z$  plane, is designed. Figure 1 shows the geometry and the P-wave velocities, although the real subsurface model parameters used by the modelling algorithm are densities and Lame coefficients.

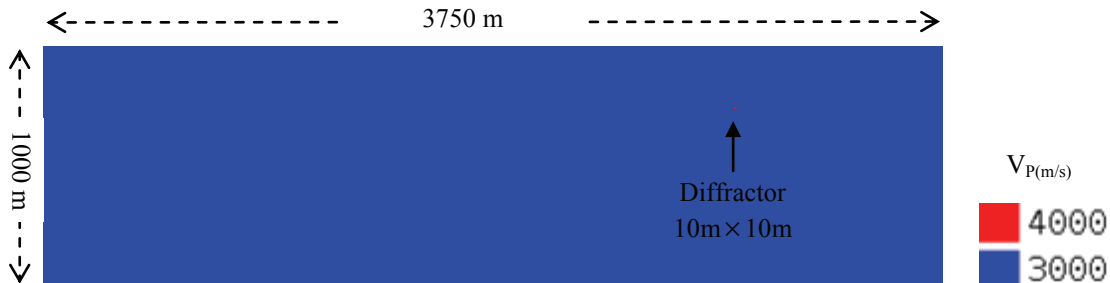


FIG. 1. A 2D subsurface model contains a point diffractor in a homogenous medium.

A rigid boundary is an idealized immovable interface. The boundary conditions are the vertical and horizontal components of displacement are zero at the boundary.

Figure 2 shows a vertical component snapshot of a rigid bottom boundary with two different amplitude scales. The top figure has a large amplitude scale. The strong waves, P-wave, S-wave, downgoing headwave, and the reflected PP-wave from the rigid bottom boundary, are displayed in grey level in proportion to their amplitudes; while the weak point diffraction can not be identified. The bottom figure has a smaller amplitude scale. The strong waves are not shown in proportion to their amplitudes, but the details of the diffraction can be identified.

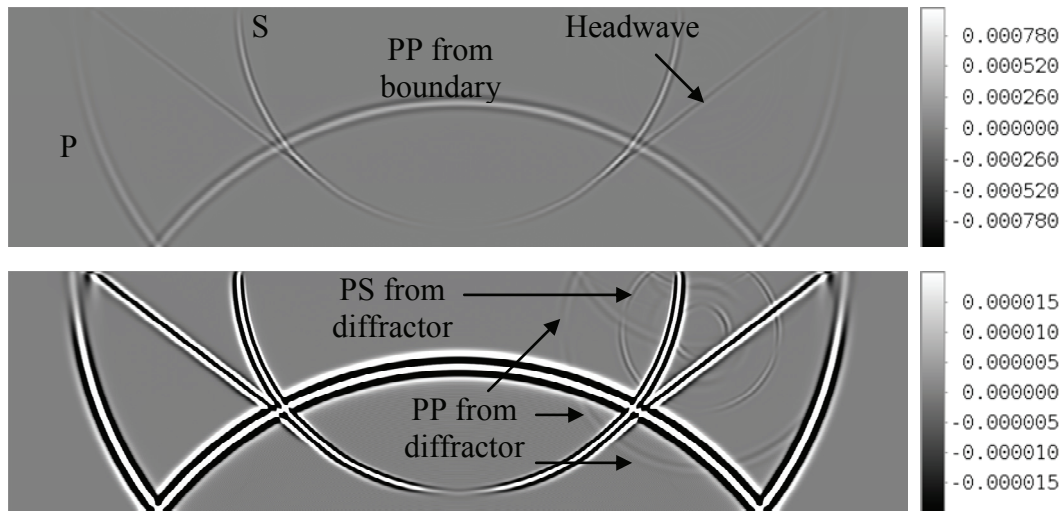


FIG. 2. A vertical component snapshot with a rigid bottom boundary shown at different amplitude scales. The top figure has a large amplitude scale, from which the weak diffraction can not be identified. The bottom one has a small scale, from which the diffraction can be identified.

### ABSORBING BOUNDARY CONDITIONS

The absorbing boundary conditions A1 (Clayton and Engquist, 1977) for the bottom boundary of a 2D elastic subsurface model can be written as

$$\begin{aligned} U_z + U_t / \beta &= 0 \\ V_z + V_t / \alpha &= 0 \end{aligned} \quad , \quad (1)$$

where  $U$  and  $V$  are, respectively, the horizontal and vertical particle velocity;  $\alpha$  and  $\beta$  are, respectively, P-wave and S-wave velocity.

Using backward difference operators with respect to  $z$  and  $t$ , system (1) in the Madariaga-Virieux staggered-grid scheme can be written as

$$\begin{aligned} \frac{U_{i,j}^{k-1/2} - U_{i,j-1}^{k-1/2}}{\Delta z} + \frac{U_{i,j}^{k+1/2} - U_{i,j}^{k-1/2}}{\beta_{i,j} \Delta t} &= 0 \\ \frac{V_{i+1/2,j+1/2}^{k-1/2} - V_{i+1/2,j-1/2}^{k-1/2}}{\Delta z} + \frac{V_{i+1/2,j+1/2}^{k+1/2} - V_{i+1/2,j+1/2}^{k-1/2}}{\alpha_{i+1/2,j+1/2} \Delta t} &= 0 \end{aligned}, \quad (2)$$

where  $(i, j)$  is the space grid index;  $k$  is the time grid index. From the formulae, particle velocities at time  $k + 1/2$  are calculated from the data at time  $k - 1/2$ .

Figure 3 shows a snapshot of the sursurface model with an absorbing bottom boundary. The reflection from the absorbing boundary is attenuated to a low level compared to the rigid boundary in Figure 2. However, the absorbing boundary reflection is still stronger than the diffractor reflection, which means that the artifacts may mask the true reflections inside the medium.

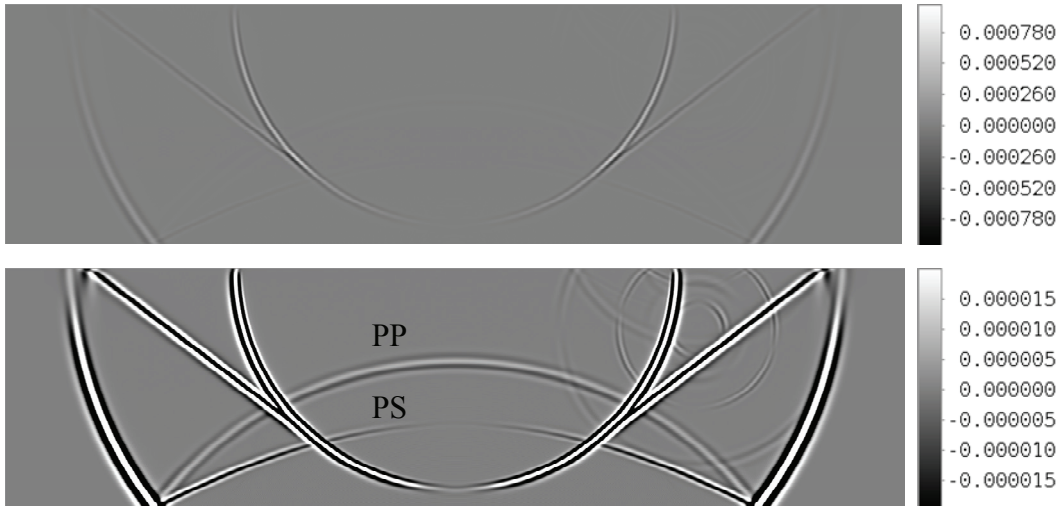


FIG. 3. A snapshot of an absorbing bottom boundary shown at different amplitude scales. The reflection from the boundary is attenuated to such a low level that it can barely identified when the snapshot is shown with a large amplitude scale (top). However, the absorbing boundary reflection is still stronger than the diffractor reflection (bottom).

### THE NONREFLECTING BOUNDARY CONDITION

A nonreflecting boundary condition (Cerjan, Kosloff, Kosloff, and Reshef, 1985) employs a strip of nodes on the boundary to attenuate wave amplitudes (Figure 5). For a strip width of  $N$  nodes, the amplitude values are multiplied by a factor

$$G = e^{-[\varepsilon(N-i)]^2}, \quad (3)$$

where  $\varepsilon$  is a constant;  $i$  denotes the grid distance between the node and the outside boundary.

Attenuating wave amplitude by the factors has two effects. Firstly, the wave is weakened towards to the outside boundary, which means the reflection from the outside boundary will be attenuated. The other effect is that, when wave enters the energy

absorbing strip, it “sees” the change in impedance of the medium and then part of the wave energy will be reflected back. Thus, for a strip width of  $N$ , there seems to exist  $N$  fictitious reflectors.

Hence, there are two kinds of reflections generated from the nonreflecting boundary. One is from the fictitious reflectors; the other one is from the outside rigid boundary. The constant  $\varepsilon$  affects both reflections. The greater the constant  $\varepsilon$  is, the stronger the fictitious reflector reflections will be, but the weaker the outside rigid boundary reflection will be. The width  $N$  has little influence on the fictitious reflector reflections, while large  $N$  certainly results in weaker outside boundary reflection.

Figure 4 shows a snapshot of a nonreflecting bottom boundary, where  $N = 50$ , and  $\varepsilon = 0.004$ . The reflections from the fictitious reflectors are comparable to the point diffractor reflection, while the reflection from the outside boundary is much stronger. (We could choose a smaller  $\varepsilon$  and a greater  $N$  to reduce both reflections to the least extent, but we choose these parameters so that we can compare the result to the next section.)

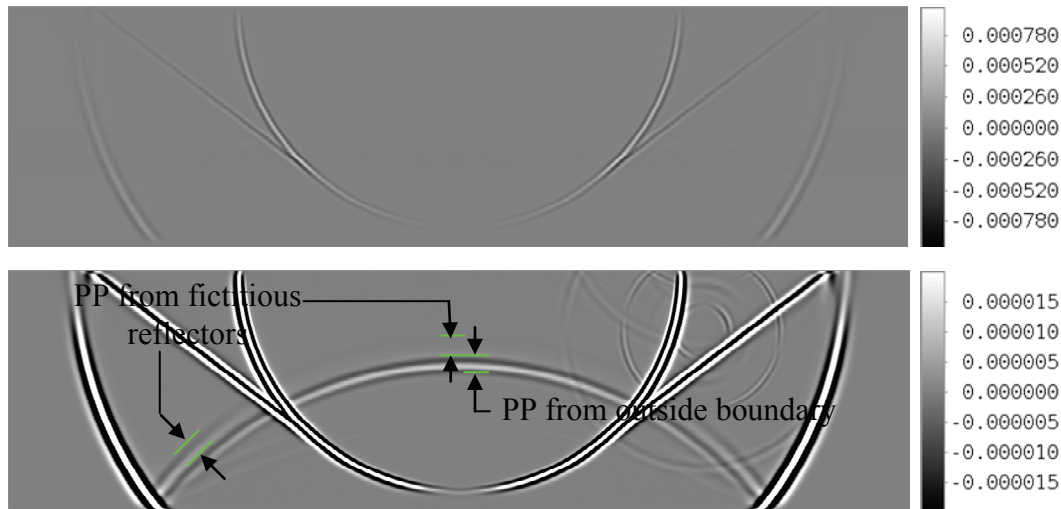


FIG. 4. A snapshot of a nonreflecting bottom boundary, where  $N = 50$ , and  $\varepsilon = 0.004$ , shown at different amplitude scales. The reflection from the boundary is attenuated to such a low level that it can barely be identified when the snapshot is shown with a large amplitude scale (top). However, it is still stronger than the diffractor reflection (bottom).

## COMBINED BOUNDARY CONDITIONS

As described in last section, the reflection from a nonreflecting boundary contains two parts. One is from the fictitious reflectors inside the attenuation strip, while the other is from the rigid boundary outside the strip. By choosing small enough  $\varepsilon$ , the fictitious reflector reflections can be controlled, however, this means a larger strip width  $N$  is needed to keep the rigid outside boundary reflection weak, which in turn, means more padding on the sides and bottom of the subsurface models and more computational cost.

By combining absorbing boundary conditions at the outside boundary of the nonreflecting boundary strip (Figure 5), with the same strip width  $N$  for the non-reflecting boundary, the boundary reflection can be reduced.

Figure 6 shows a snapshot of the combined boundary, where  $N = 50$ , and  $\varepsilon = 0.004$  for the nonreflecting strip. Comparing to Figure 4, the reflection from the bottom boundary is much more attenuated. (The same as mentioned at last section, we choose these parameters for the sake of algorithm demonstration. we could choose smaller  $\varepsilon$  and greater  $N$  to reduce the resident reflections to the least extent.)

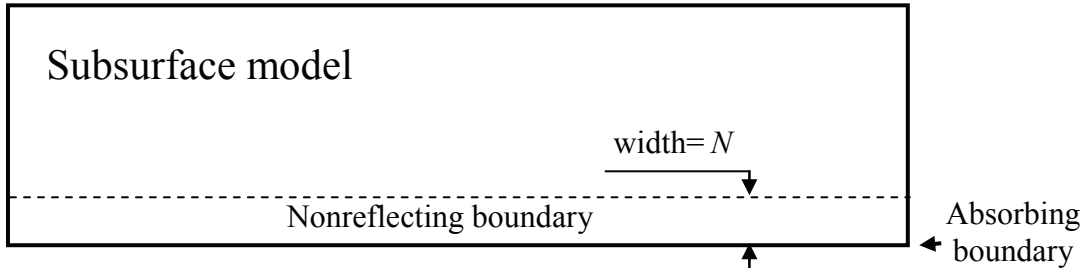


FIG. 5. Combining a nonreflecting and an absorbing boundary condition at the bottom of the subsurface model.



FIG. 6. A snapshot with a combined boundary of nonreflecting and absorbing at the bottom of the model, where  $N = 50$ , and  $\varepsilon = 0.004$  for the nonreflecting strip.

## CONCLUSIONS

The absorbing boundary conditions reduce computational edge artifacts into a low level, but the artifacts still might mask weak reflector reflections.

The nonreflecting boundary condition produces two parts of reflections: one is from the attenuation strip which works like fictitious reflectors; the other one is from the outside boundary. To reduce both reflections, the nonreflecting strip needs to be wide, and this leads to more computational cost.

Combining the absorbing boundary conditions with the nonreflecting boundary condition results in less boundary artifacts with little additional computational cost.

## ACKNOWLEDGEMENTS

The authors gratefully acknowledge the support of CREWES sponsor companies and various CREWES staff and students.

## REFERENCES

- Cerjan, C., Kosloff D., Kosloff, R., and Reshef, M., 1985, A nonreflecting boundary condition for discrete acoustic and elastic wave equations, *Geophysics*, **50**, 705-708.
- Clayton, R., and Engquist, B., 1977, Absorbing boundary conditions for acoustic and elastic wave equations, *bulletin of the Seismological Society of America*, **67**, 1529-1540.
- Clayton, R. and Engquist, B., 1980, Absorbing boundary conditions for wave-equations migration, *Geophysics*, **45**, 895-904.
- Engquist, B. and Majda, A., Absorbing boundary conditions for numerical simulation of waves, *Proc. Natl. Acad. Sci. USA*, **74**, 1765-1766.
- Collino, F., and Tsogka, C., 2001, Application of the perfectly matched absorbing layer model to the linear elastodynamic problem in anisotropic heterogeneous media, *Geophysics*, **66**, 294-307.
- Long, L.T., and Liow J.S., 1990, A transparent boundary condition for finite-difference wave simulation, *Geophysics*, **55**, 201-208.
- Virieux, J., 1986. P-SV wave propagation in heterogeneous media: velocity-stress finite-difference method, *Geophysics*, **51**, 889-901.